

Organic & Biomolecular Chemistry

Accepted Manuscript



This is an *Accepted Manuscript*, which has been through the Royal Society of Chemistry peer review process and has been accepted for publication.

Accepted Manuscripts are published online shortly after acceptance, before technical editing, formatting and proof reading. Using this free service, authors can make their results available to the community, in citable form, before we publish the edited article. We will replace this *Accepted Manuscript* with the edited and formatted *Advance Article* as soon as it is available.

You can find more information about *Accepted Manuscripts* in the [Information for Authors](#).

Please note that technical editing may introduce minor changes to the text and/or graphics, which may alter content. The journal's standard [Terms & Conditions](#) and the [Ethical guidelines](#) still apply. In no event shall the Royal Society of Chemistry be held responsible for any errors or omissions in this *Accepted Manuscript* or any consequences arising from the use of any information it contains.

Enthalpy-driven Nuclease-like Activity and Mechanism of Peptide-Chlorambucil Conjugates

Robin C.K. Yang,¹ Jonathan T.B. Huang,¹ Yu-Ling Chen,¹ Chia-Chun Hung,¹ Mokai Liao,¹ Wen-Chen Yao,¹ Chiu-Heng Chen,¹ Chien-Chung Liou,¹ Michael J. Waring,² and Leung Sheh^{1*}

¹Department of Chemistry and Life Science Center, Tunghai Christian University, Taichung, Taiwan 407, R.O.C., ²Department of Pharmacology, University of Cambridge, Tennis Court Road, CB2 1PD, England.

R.C.K.Y. and J.T.B.H. contributed equally to this work

*To whom correspondence should be addressed. Tel: +886-4-23592674;

fax: +886-4-23590426; E-mail: Lsheh@thu.edu.tw

We report the results of attaching the anticancer drug chlorambucil (CLB) to two high-affinity DNA binding peptides: Met-Hyp-Arg-Lys-(Py)₄-Lys-Arg-NH₂ (HyM-10) and Gln-Hyp-Arg-Lys-(Py)₄-Lys-Arg-NH₂ (HyQ-10). These CLB-peptide conjugates cleave DNA very effectively and sequence-selectively without the adjuvant use of chemicals, heat, or UV irradiation. Polyacrylamide gel electrophoresis identifies the sites where CLB-HyM-10 and CLB-HyQ-10 attack a complementary pair of 5'-³²P-labeled duplexes derived from pBR322 in the absence of piperidine or other chemical additives. Matrix-assisted laser desorption ionization time-of-flight mass spectrometry (MALDI-TOF-MS) has confirmed the preferential cleavage sites as well as a novel stepwise cleavage mechanism of sequence-selective DNA cleavage. Resembling restriction endonucleases, the CLB-peptide conjugates appear to be capable of producing double strand DNA breaks. Circular dichroism studies show that CLB-HyM-10 and CLB-HyQ-10 induce significant local conformational changes in DNA via the minor groove, possibly with dimeric binding stoichiometry. The energetic basis of DNA binding by these conjugates has been investigated by isothermal titration calorimetry, revealing that the binding of both the peptides and their CLB conjugates is overwhelmingly enthalpy-driven. The maintenance of a conserved negative binding free energy

in DNA-conjugate interactions is a crucial feature of the universal enthalpy-entropy compensation phenomenon. The strongly enthalpy-driven binding of CLB-peptide conjugates to preferred loci in DNA furnishes the required proximity effect to generate the observed nuclease-like sequence-selective cleavage.

1 Introduction

The design and synthesis of sequence-selective chemical nucleases is an important topic in the application of chemistry to biological and medical sciences. Most DNA cleavage agents or chemical nucleases are metal complexes that mediate strand cleavage via various reactive oxygen species.¹⁻⁴ Others which operate by photo-cleavage require strong UV irradiation to generate free radicals.⁵ It has long been the aspiration of chemists and bioorganic researchers to design and synthesize chemical nucleases that are capable of cleaving nucleic acids with sequence specificity mimicking that of restriction enzymes, free from the limitations imposed by chemical additives and/or UV irradiation.

Chlorambucil (CLB) is an anticancer drug widely used in clinical practice against chronic lymphocytic leukemia, non-Hodgkins lymphoma, and other types of cancer.⁶⁻⁷ CLB alkylates DNA preferentially at the guanine-N7 position. However, CLB and CLB-peptide conjugates do not generally cleave DNA in the absence of additives like piperidine. In 1995, we reported the synthesis of cyclic peptide-chlorambucil conjugates endowed with DNA-alkylating activities that could cleave DNA in the presence of piperidine.⁸ We also synthesized dipeptide conjugates that were disubstituted with chlorambucil and a 2,6-dimethoxyhydroquinone derivative, albeit requiring ferrous ions or high temperature (thermal cleavage) to

elicit DNA cleavage.⁹

Recently, we found that when chlorambucil is conjugated to certain arginine-containing peptides, the conjugate is capable of cleaving DNA at 37°C or room temperature in the absence of piperidine or other cleavage additives. Early studies commenced with the attachment of chlorambucil to a peptide with weak DNA binding ability to afford the conjugate: CLB-Asn-Arg-Arg-Ala-Asn-Ala-NH₂ (CLB-NR6). Although the parent peptide Asn-Arg-Arg-Ala-Asn-Ala-NH₂ (NR6) did not prove positive in DNA footprinting studies,¹⁰ its CLB-conjugate did show remarkable DNA cleavage in the absence of chemical additives (Figure 1A). In search of CLB-conjugates with higher DNA sequence-selective cleavage capabilities, we went on to attach CLB to two designed peptides incorporating the XP(Hyp)RK motif: Met-Hyp-Arg-Lys-(Py)₄-Lys-Arg-NH₂ (HyM-10) and Gln-Hyp-Arg-Lys-(Py)₄-Lys-Arg-NH₂ (HQ-10). Peptides incorporating such motifs possess excellent DNA binding capability in the sub-micromolar concentration range.¹¹⁻¹⁶ Further attachment of one or more 4-amino-1-methylpyrrole-2-carboxylic acid residues (Py) to XP(Hyp)RK peptides enhances their sequence-specificity toward sequences containing consecutive arrays of A or T nucleotides.^{11,14-16}

Here we report that peptides HyM-10 and HQ-10 bind satisfactorily to DNA in a sequence-selective manner as assessed by DNase I footprinting. Polyacrylamide gel

electrophoresis is ideal for exploring sequence-selectivity of DNA cleavage by the CLB-peptide conjugates CLB-HyM-10 and CLB-HyQ-10. In addition, circular dichroism and isothermal titration calorimetry are employed to investigate induced DNA conformational changes as well as the thermodynamic aspects of CLB-peptide conjugate-DNA interactions, respectively. Recall that the energetic basis of general DNA-peptide interactions has been discussed in detail recently.¹⁶ We have also used matrix-assisted laser desorption ionization time-of-flight mass spectrometry (MALDI-TOF-MS) to investigate preferential cleavage sites as well as the mechanism of DNA cleavage by these conjugates.

2. Results and discussion

Early DNA cleavage studies were carried out using the conjugate CLB-Asn-Arg-Arg-Ala-Asn-Ala-NH₂ (CLB-NR6). The design of the peptide portion NR-6 (Asn-Arg-Arg-Ala-Asn-Ala-NH₂) was derived from residues 30-35 of tumor necrosis factor- α (TNF α).¹⁷ Peptide NR-6 alone produced agarose gel retardation as well as some DNA nicking effects on pBR322 plasmid. However, it did not produce any DNase I footprints on test DNA duplexes,¹⁰ suggesting that its binding to DNA must be quite weak. On the 135-mer lower strand of pBR322 the CLB-peptide conjugate CLB-NR6 produced efficient DNA cleavage in the absence of piperidine or other cleavage additives (Figure 1A). The cleavage by CLB-NR6 is not particularly

sequence-selective at high concentrations but is more evidently selective at lower concentrations (500-1000 nM), notably at two loci: positions L89-87 and L114-112, both comprising the sequence 5'-GGT-3' (Figure 1A).

Next, we conjugated chlorambucil to the *N*-terminal of the peptide carboxamide Met-Hyp-Arg-Lys-(Py)₄-Lys-Arg-NH₂ (HyM-10) which is endowed with strong DNA sequence-selective binding to d(AAAA)-d(TTTT) or d(AAA)-d(TTT) . The resulting conjugate CLB-Met-Hyp-Arg-Lys-(Py)₄-Lys-Arg-NH₂ (CLB-HyM-10) induced significant DNA cleavage at four major sites on the lower strand at positions L80-78, L87-85, L92-88, L101-96 and L115-111, corresponding to the sequences 5'-CAC-3', 5'-TAT-3', 5'-TGCGGTA-3', 5'-ACGCA-3', and 5'-GGTA-3' (Figure 1B, Figure 2 and Table 1). Notably, on the 135-mer lower strand, conjugate CLB-HyM-10 produces sequence-selective cleavages at position L80-78, corresponding to the sequence 5'-CAC-3', position L88-86, comprising the sequence 5'-GTA-3', and position L114-112, corresponding to the sequence 5'-GGT-3'. It is striking that the cleavage site around position L80-78 containing the sequence 5'-CAC-3' disappears at conjugate concentration higher than 1000 nM (Figure 2); this result is fully reproducible when the experiment is repeated.

A strong cleavage site also occurs around position L72-68 but was truncated in the autoradiograph. On the other hand, four major DNA cleavage sites are found at the

upper strand positions: U76-80, U81-85, U98-106, and U107-110, corresponding to the sequences 5'-CGGTG-3', 5'-TGAAA-3', 5'-GCGTAAGGA-3', and 5'-GAAAA-3' (Table 1). The most pronounced cleavage sequences in the lower strand appear to be 5'-GGTA-3', and 5'-ATG-3'. However, it is notable that an unusual cleavage sequence also occurs in the lower strand: 5'-CAC-3'. On the other hand, the strongest cleavage sequences in the upper strand appear to be 5'-GGAG-3' and 5'-AAAA-3'. Comparing the sequence-binding preferences from footprinting studies (Figure 1C, Figure 2) and the sequence cleavage preferences (Figure 1B, Figure 2), it appears that there are correlations. On the upper strand, the sequence preferences of peptide HyM-10 correspond to U84-90 and U104-115 whereas the corresponding cleavage by CLB-HyM-10 occurs at U81-85, with common loci of 5'-AAA-3' and 5'-GAAAA-3', respectively. This implies that the cleavage preference of conjugate CLB-HyM-10 on the upper strand is directed by preliminary sequence-selective binding of the peptide portion of the conjugate to DNA. The correlation between binding and cleavage on the lower strand is much weaker; only one common locus is found at position L82-80, corresponding to the sequence 5'-CAC-3'. The sequence-selective cleavage pattern seen with the CLB-peptide conjugate CLB-Gln-Hyp-Arg-Lys-(Py)₄-Lys-Arg-NH₂ (CLB-HyQ-10) (Figure 1D, 1E, text; Supporting Information [I]) appears to be similar to that of conjugate

CLB-HyM-10.

We envisage that the peptide moieties of the conjugate molecules interact with the recognition motifs d(AAAA)-d(TTTT) or d(AAA)-d(TTT) in the DNA minor groove via monodentate, interstrand bidentate,^{14,15,18} ionic and hydrophobic interactions. The position of DNA cleavage is expected to lie close to the CLB moiety. However, the observed site of cleavage is often rather wide, ranging over as many as 5-9 bases since the conjugate may bind fairly selectively to quite a wide binding locus. Nevertheless, the peptide-directed sequence recognition must surely underlie the proximity effect directing the CLB moiety to the preferred cleavage site(s). It is also possible that the conjugate molecules may bind to recognition motifs in the duplex in dimeric form, either simultaneously or as monomers at close intervals.

To investigate the stoichiometry and possible conformational changes associated with the peptide-DNA interactions, a 13-mer deoxyribonucleotide duplex d(TAGGAGAAAATAC)-d(GTATTTTCTCCTA) (U4A-L4T) corresponding to the recognition site in the pBR322 fragments at position 103-114 was used as a substrate for CD studies. On raising the concentration of peptides HyM-10 (Figure 3A) or HyQ-10 (Supporting Information [II]) added to duplex U4A-L4T, a near-isoelliptic point around 280 nm was identified, suggesting a predominantly two-component binding process. This reflects the development of a strong, broad dose-dependent CD

enhancement around 330 nm, clearly visible in the difference spectrum (Fig 3B) for the conjugates CLB-HyM-10 and CLB-HyQ-10 as well.

A number of previous articles^{19,20} have demonstrated that molecules which bind in the minor groove of DNA typically induce the appearance of a positive CD band around 320 nm. The same seems to be the case for the peptides and CLB conjugates studied here. Previous studies have also indicated that at ligand/DNA ratios between 0.5 and 2.0 most likely one molecule of each peptide binds to loci such as d(AAAA)-d(TTTT) in the minor groove, as suggested by a hint of a small plateau, while at ratios between 2 and 3 further small plateau regions can be tentatively discerned, suggesting that two molecules can bind in a dimeric fashion to the minor groove. As the [ligand]/[duplex] ratio rises above 3 progressive increases in $\Delta\theta$ suggest that further ligand molecules start to bind non-specifically – probably to the wide major groove. All these features are apparent in the CD behavior of the peptides and conjugates reported here (Figures 3A-E, text; Figure [II], Supporting Information). In this study, Job's plots (Figure 3E) show that the ligand/DNA ratio of peptide HyM-10 and its conjugate CLB-HyM-10 is 3:1 whereas that of HyQ-10 and CLB-HyQ-10 is 2:1. It is likely that peptide HyM-10 and its conjugate bind to the oligonucleotide duplex U4A-L4T rather non-selectively at higher ligand concentration, a common DNA-binding property shared by many of our synthetic peptides

incorporating the XP(Hyp)RK motif.¹³⁻¹⁵

Although the mechanism of DNA cleavage by established alkylating agents is generally understood, much less is known about the complex mechanisms of action of designed agents. To gain insight into the sequence-selective DNA cleavage mechanism of CLB-peptide conjugates we carried out MALDI-TOF analyses of the cleavage fragments produced from a double-stranded oligonucleotide duplex d(TAGGAGAAAATAC)-d(GTATTTTCTCCTA) (U4A-L4T), employing 3-hydroxy-picolinic acid/picolinic acid/ammonium citrate or trihydroxyacetophenone/ammonium citrate as matrix. Another oligonucleotide duplex was also employed in MALDI-TOF analyses: d(AAGGAGAAAATAC)-d(GTATTTTCTCCTT) (XU4A-XL4T). The sequence of this duplex was designed to verify the site of cleavage when two or more cleavage fragments have the same calculated mass.

MALDI-TOF analyses confirm that significant sequence-selective cleavage of the oligonucleotide duplexes occurs after incubation with CLB-HyM-10 or CLB-HyQ-10 for 15-30 min at room temperature or 37°C, in the complete absence of special chemical additives. The CLB-peptide conjugates can also cleave single strand oligonucleotides (data not shown) as well as double strand oligonucleotides. The cleavage of CLB-HyM-10 and CLB-HyQ-10 on the U4A-L4T duplex (Figure 4,

A,B,E,F, text; Figure [III], A,B, Supporting Information) is much less sequence-selective than that on the XU4A-XL4T duplex (Figure 4, C,D, text; Figure [III], C,D, Supporting Information). The major cleavage fragments most frequently detected (i.e. those observed at least twice in different duplex/CLB-peptide conjugate reactions) are shown in Table 2, where the preferential sites of cleavage and corresponding cleavage mechanisms are proposed. Two routes to hydrolysis of the phosphodiester bond may be involved: depurination or depyrimidination. For DNA glycosylase, depurination involving an oxocarbenium intermediate that leads to subsequent hydrolytic cleavage of the 5'- or 3'-phosphodiester bonds is well characterized.²¹ Since our CLB-peptide conjugates can induce significant depurination and depyrimidination with concomitant cleavage of the phosphodiester bond, a similar DNA cleavage mechanism is proposed in Figure [IV], Supporting Information. In addition, a mechanism of phosphodiester hydrolysis by thymidine phosphorylase via depyrimidination of thymine has recently been reported as a concerted bimolecular process, involving nucleophilic attack of the 2-deoxyribose oxocarbenium ion.²² In Table 2, the Maldi-tof ms peaks 998, 1948, 2337, 2643 reveal corresponding oligonucleotide fragments preserving purine or pyrimidine base on the 5'- and 3'- ends. However, depurination and depyrimidination may occur on

the 5'- or 3'- end of the adjacent fragment originally linking the cleaved fragment, causing hydrolysis of corresponding phosphodiester bonds.

To interpret the sequence-selective cleavages we propose an initial binding alignment of the peptide-CLB conjugate with the oligonucleotide duplex (Figure 5A-D). The peptide moiety of the conjugate first interacts with the recognition locus d(AAAA)-d(TTTT) in the DNA minor groove via monodentate and interstrand bidentate hydrogen bond interactions, supported by ionic and hydrophobic interactions, and thus the CLB moiety is positioned close to certain DNA loci. After tight binding, the resultant phosphodiester bond cleavage must be dominated by proximity to the CLB moiety, which mediates depurination or depyrimidination of a base leading to subsequent hydrolysis of the DNA backbone.

The use of the XU4A-XL4T duplex unambiguously verifies the site of cleavage as well as confirming the validity of the assignment of the cleavage fragments. For example, the 5'-end nucleotide on the upper strand of U4A-L4T is T₁ whereas that of XU4A-XL4T is A₁ (Figure 4, A-D). The cleavage fragments induced by conjugate CLB-HyQ-10 are f₁(mass 1442.2) and c₃(mass 2177.6) from the upper strand of U4A-L4T, corresponding to the fragments f₁(mass 1451.2) and c₃(mass 2186.9) from the upper strand of XU4A-XL4T (Figure 4B,D), respectively, indicating that the site of phosphodiester bond cleavage by the CLB-peptides on different duplexes that differ by

a single nucleotide is the same.

Figures 5A-5D illustrate a novel “stepwise cleavage mechanism” of the DNA duplex by conjugate CLB-HyM-10 or CLB-HyQ-10 on the U4A-L4T duplex. The proposed mechanisms explained by successive association and dissociation processes directing the proximity of the CLB moiety to another susceptible base, producing depurination or depyrimidination, and generating smaller fragments after each cut. For conjugate CLB-HyM-10, different binding alignment of a single CLB-HyM-10 molecule with the duplex would result in the removal of 5'-T₂₅-A₂₆-3' by depyrimidination of T₂₅ and also the truncating of 5'-G₁₄-T₁₅-A₁₆-3' by depurination of A₁₆ (Figure 5A). Next, binding of two molecules of the CLB-peptide conjugate in dimeric fashion to this truncated duplex locates a CLB moiety close to preferred sites and initiates cleavage of the duplex releasing four or five single strand fragments. Depurination of A₅ or G₆ in the upper strand, depyrimidination of T₂₂ and T₂₀ of the lower strand are indicated by the production of fragments from opposite strands: 5'-T₁-A₂-G₃-G₄-A₅-dr-3' (mass 1732.3); and cleaved fragments: 5'-T₁₇-T₁₈-T₁₉-T₂₀-C₂₁-3' (mass 1597.9) and 5'-T₁-A₂-G₃-G₄-dr-3' (mass 1442.2) (Figure 5A). The fragment 5'-T₁₉-T₂₀-C₂₁-T₂₂-C₂₃-C₂₄-dr-3' (2033.1) is generated by alignment of the CLB conjugate to the duplex near T₁₈, causing depyrimidination of this nucleotide and subsequent hydrolysis of the 5'-T₁₈-T₁₉-3' phosphodiester bond (Figure 5A). Stepwise cleavage of the upper strand or lower strand

initiated by successive binding by a single molecule of this conjugate to a preferred cleavage site afford other major fragments: 5'-G₄-A₅-G₆-A₇-A₈-A₉-A₁₀-3' (2337.3), 5'-A₂-G₃-G₄-A₅-G₆-A₇-A₈-A₉-3' (2643.2), and 5'-G₁₄-T₁₅-A₁₆-3' (998.3).

Similarly, binding alignment of a single molecule of conjugate CLB-HyQ-10 to duplex U4A-L4T first removes the dinucleotide 5'-G₁₄-T₁₅-3' or a G₁₄ nucleotide from the lower strand, followed by dimeric binding of two molecules that initiates cleavage to afford fragments from opposite strands: 5'-T₁-A₂-G₃-G₄-A₅-dr-3' (mass 1732.7); 5'-T₁-A₂-G₃-G₄-dr-3' (mass 1442.3), and 5'-T₁₅-A₁₆-T₁₇-T₁₈-T₁₉-T₂₀-3' (mass 1948.6) (Figure 5B, text; Table [Ia], [Ic], Supporting Information). Similar to the cleavage mechanism of CLB-HyM-10, the fragment 5'-T₁₉-T₂₀-C₂₁-T₂₂-C₂₃-C₂₄-dr-3' (2033.9) is generated by depyrimidination of nucleotide T₁₈ and subsequent hydrolysis of the 5'-T₁₈-T₁₉-3' phosphodiester bond. Stepwise cleavage of the upper strand or lower strand triggered by successive monomeric binding to a preferred site generate some other major fragments: 5'-G₄-A₃-G₆-A₇-A₈-A₉-A₁₀-3' (2337.5), 5'-A₂-G₃-G₄-A₅-G₆-A₇-A₈-A₉-3' (2642.6), 5'-G₁₄-T₁₅-A₁₆-3' (998.3), 5'-A₁₀-T₁₁-3' (712.4), 5'-T₁₅-A₁₆-T₁₇-T₁₈-T₁₉-T₂₀-C₂₁-T₂₂-C₂₃-dr-3' (2943.7), and 5'-A₅-G₆-A₇-3' (970.7).

Further supports of the stepwise cleavage mechanism are presented by the cleavage of duplex XU4A-XU4T by conjugates CLB-HyM-10 and CLB-HyQ-10 (Figures 5C, D). In

these cleavage events the mechanism follows the general stepwise cleavage pattern: an initial truncation of an upper or lower strand of the DNA duplex by a single molecule of the CLB-peptide conjugate with repetitive binding to recognition sites. Subsequently, dimeric binding of the conjugate CLB-HyM-10 triggers the cleavage of 5'-A₁-A₂-G₃-G₄-A₅-G₆-A₇-3' (2186.9) and two fragmental pairs from opposite strands : 5'-A₇-A₈-A₉-A₁₀-T₁₁-A₁₂-3' (1960.3) and 5'-T₁₅-A₁₆-T₁₇-T₁₈-T₁₉-T₂₀-3' (1948.5). The fragment 5'-T₁₇-T₁₈-T₁₉-T₂₀-C₂₁-3' (1597.9) was produced by truncating 5'-T₁₅-A₁₆-3' from the lower strand followed by depyrimidination of T₂₂ to cleave the 5'-C₂₁-T₂₂-3' phosphodiester bond (Figure 5C). By a similar mechanism, conjugate CLB-HyQ-10 induces the generation of fragmental pairs 5'-A₁-A₂-G₃-G₄-A₅-G₆-A₇-3' (2186.6) and 5'-T₁₉-T₂₀-C₂₁-T₂₂-C₂₃-C₂₄-dr-3' (2033.9), and fragment 5'-G₄-A₅-G₆-A₇-A₈-A₉-3' (2024.8) (Figure 5D).

Some evidences of generation of double strand DNA breaks are demonstrated cleavage experiments on the XU4A-XL4T duplex (Figure 5C, D). Typical fragmental pairs from opposite strands of duplex XU4A-XL4T are produced by conjugate CLB-HyM-10 : 5'-A₇-A₈-A₉-A₁₀-T₁₁-A₁₂-3' (1960.3) and 5'-T₁₅-A₁₆-T₁₇-T₁₈-T₁₉-T₂₀-3' (1948.3) (Table [Ib], Supporting Information). Similarly, fragmental pairs from opposite strands of duplex XU4A-XL4T are generated by conjugate CLB-HyQ-10: 5'-A₁-A₂-G₃-G₄-A₅-G₆-A₇-3' (2186.6) and

5'-T₁₉-T₂₀-C₂₁-T₂₂-C₂₃-C₂₄-dr-3' (2033.9) (Table [Id], Supporting Information). We reason that the CLB-peptide conjugates are capable of generating double strand DNA breaks when the CLB moiety is repeatedly located near the preferred cleavage points.

We suggest that the stepwise cleavage mechanism points to a general feature: the truncation of an upper or lower strand can be initiated by binding of a single molecule of the CLB-peptide conjugate. Next, monomeric binding of the conjugate may produce more fragments whereas dimeric binding of the conjugate to the DNA duplex may generate fragmental pairs from opposite strands, producing double strand breaks in the meantime. Stepwise cleavage of the duplex DNA can often be achieved by binding of a single molecule of the CLB-peptide conjugate repeatedly to various recognition sites, yielding different fragments.

The energetic basis of general DNA-peptide interactions was discussed in detail recently.¹⁶ To gain insight into the thermodynamic basis of DNA binding and cleavage by peptides incorporating the XHypRK motif as well as the corresponding CLB conjugates, isothermal calorimetry titration studies (ITC) were carried out (Figures 6A, 6B). Plots of heat versus molar ratio were obtained by subtracting the heat of dilution for the addition of peptide or conjugate into buffer. In both CD and ITC experiments, the titrations were performed by adding a small aliquot of CLB-peptide conjugate to bulk DNA solution, so the corresponding detection of ellipticity changes and enthalpy changes

may be limited to relatively short periods of DNA-ligand binding, that is, DNA binding must precede DNA cleavage. CD spectra of CLB-peptide conjugates titrated into DNA reveal significant concentration-dependent ellipticity increases around 330 nm, suggesting that the CLB-peptide conjugates bind tightly to the intact minor groove of DNA. If the DNA is already cleaved, no corresponding minor groove may be available for the concentration-dependent binding of CLB-peptide conjugates. Thus, we reason that the ellipticity changes (CD) and enthalpy changes (ITC) reflect primary binding interactions of the CLB-peptide conjugate with intact DNA rather than with nicked DNA, although we do not preclude the possibility that some DNA was cleaved during ITC and CD experiments.

The ITC results indicate that either the peptide or the CLB-conjugates prefers to bind in a dimeric fashion to d(AAAA)-d(TTTT) sites. In Breslauer's pioneering study of the binding of netropsin, distamycin, ethidium and daunorubicin to duplex poly[dA-dT].[dA-dT], the ΔH values lay within the range -8.9 to -18.5 kcal mol⁻¹.²³ In comparison, the negative enthalpy changes for binding of the peptide and its CLB conjugate incorporating the XHypRK motif to DNA are significantly greater at their preferred DNA binding sequences (ΔH lies within the range -25.4 to -74.4 kcal mol⁻¹; Table 3). Thus, the ITC results indicate that binding of the peptides and CLB-peptide conjugates to DNA is overwhelmingly enthalpy-driven. However, the opposing entropic

effects for all of the peptides and CLB-peptide conjugates are very unfavorable: $T\Delta S$ falls within the range -17.8 to -65.9 kcal mol⁻¹ (Table 3).

The unusually strong exothermic enthalpy change could be due to the formation of ionic interactions between the side chains of basic residues like Arg and Lys with the DNA phosphates as well as the interstrand bidentate interactions formed between the side chains of Met, Arg, and Lys of peptides with the O2 of thymine and N3 of adenine, as will be considered below. First it should be noted that the peptides and their corresponding chlorambucil conjugates clearly exhibit the enthalpy-entropy compensation (EEC) phenomenon that has been described before (Figure 6B). Figure 6C shows a plot of ΔH versus $T\Delta S$ for four peptides and four CLB-peptide conjugates. The linearity of ΔH versus $T\Delta S$ for these eight ligands is impressive: slope = 1.0155; y -intercept = -7.9 kcal mol⁻¹. A 3-dimensional figure of ΔH , $T\Delta S$ and ΔG can be plotted to emphasize the linear enthalpy-entropy-free energy relationship that underlines the EEC phenomenon in DNA-small ligand interactions (Figure 6D). A near-straight line is suspended in thermodynamic space, with ΔG values maintained within an almost constant range around -7.9 kcal mol⁻¹.

In a recent study¹⁶ as well as the work reported here, we have put forward the view that strong exothermic enthalpy is needed to overcome the very unfavorable entropy required to attain efficient binding to DNA. In many cases, when a protein²⁴ or a peptide

bind to DNA, cations from the DNA are released to bulk solution, the increase in entropy from solvent reorganization $\Delta S^\circ_{\text{H}}$ (hydrophobicity) and $\Delta S^\circ_{\text{ions}}$ (polyelectrolyte) favor DNA-ligand binding. However, the sum of entropy change $\Delta S^\circ_{\text{rt}}$ (rotation and translation), $\Delta S^\circ_{\text{vib}}$ (vibration) and $\Delta S^\circ_{\text{conf}}$ (configuration) are typically negative and oppose to binding, resulting in a decrease in total entropy.²⁴ Ionic interactions between the positively charged Arg and Lys side chains of the peptides or conjugates and internucleotide phosphates probably restrict the conformational mobility of the DNA duplex and may account for the dramatic decrease in total entropy. According to the law of conservation of energy, any loss in entropic energy must transform to exothermic energy, which in turn causes an increase in enthalpy. We envisage that high exothermic energy is required for allosteric adjustment of DNA conformation within the binding loci by means of hydrogen bonding and ionic interactions between DNA duplex and peptide,¹⁶ augmenting the favorable energy components ΔG_{h} , $\sum \Delta G_{\text{p}}$, ΔG_{conf} , and ΔG_{vdw} in Williams' equation,²⁵ and facilitating positively cooperative binding of approaching peptide or CLB-peptide molecules. These considerations formalize a situation in which the strongly negative binding enthalpy for these peptides and CLB-conjugates is required for the compensation of energy, sustaining an acceptable negative value of net binding free energy ΔG mandatory for DNA-ligand interactions.

3. Conclusion

This study shows that chlorambucil-peptide conjugates elicit significant sequence-selective cleavage of DNA without the chemical additives or thermal assistance that are usually required for chemical nucleases. Gel electrophoresis experiments reveal that although the cleavage sites are mostly adjacent to A's and G', some sequence-selective cleavages also occur on the 5'- or 3'- sides of pyrimidines such as 5'-CAC-3', 5'-CGGTG-3' and 5'-TGAA-3'. MALDI-TOF studies of cleavage fragments from duplexes U4A-L4T and XU4A-XL4T indicate preferential cutting at comparable sites. Notably, MALDI-TOF studies of conjugates CLB-HyM-10 and CLB-HyQ-10 versus the two DNA duplexes, a total of four reactions, all point to a novel stepwise scissioning mechanism. Generation of a particular sequence-selective cleavage fragment can often be interpreted as resulting from binding of the CLB-peptide conjugate to its cognate recognition site on DNA so as to place the CLB moiety close to a susceptible base, causing depurination or depyrimidination, and inducing the hydrolysis of a phosphodiester bond, generating smaller fragments after each cut. The general features of the stepwise scissioning mechanism are: following initial truncating an upper or lower strand of the DNA duplex by a single molecule of the CLB-peptide conjugate, monomeric binding of the conjugate may produce more fragments whereas dimeric binding of the conjugate to the DNA duplex may generate

fragmental pairs from opposite strands, producing double strand breaks in the meantime.

It also appears that the binding of CLB-peptide conjugates to the recognition locus on DNA is overwhelmingly enthalpy-driven. The strongly negative binding enthalpy measured for these peptides and conjugates is evidently required for a process of energy compensation, needed to sustain an acceptable negative value of net binding free energy. We believe that this strongly enthalpy-driven binding of the peptide conjugate to DNA underlies the proximity effect that positions the CLB moiety close to the preferred cleavage site, manifested in the observed nuclease-like sequence-selective cleavage.

The highly effective cleavage of DNA by the CLB-peptide conjugates that we have described, in the absence of U.V. irradiation, chemical additives or thermal assistance, mimics the action of natural nucleases. To our knowledge, this new series of CLB-peptide conjugates is one of the most effective sequence-selective chemical nucleases reported. As such, the conjugates and their congeners merit further investigation.

Acknowledgements

We thank professors L.S. Kan, D.K. Chang, S.T. Chen, S.H. Wu and Y.T. Tau, Academia Sinica, for helpful advice and access to ITC and CD facilities. We also thank professors Lin Ma, C.C. Cheng, Y.J. Chen and C.W. Ong for encouragement and helpful advice.

This work was supported by grant NSC97-2113-M029-005 and funds from Tunghai Christian University and the Jeng Ching Ho Foundation.

4 Experimental

4.1 Chemicals and biochemicals: All the protected amino acid derivatives were purchased from AnaSpec, Inc. (San Jose, CA) and all peptides are synthesized in our laboratory. All other analytical reagents were purchased from Acros, Tedia or Sigma. Melting points were determined on a Mel-Temp apparatus (Cambridge, Mass) and are uncorrected. Optical rotations were determined on a Rudolph Autopol II instrument. Radiolabeled nucleoside triphosphates [γ - ^{32}P]dATP were obtained from NEN Life Science Products at a specific activity of 6000 Ci/mmol. *Taq* polymerase, T4 polynucleotide kinase, and DNase I were purchased from Promega. All of the biochemicals were used according to the supplier's recommended protocol in the activity buffer provided. Other chemicals were analytical grade reagents, and all solutions were prepared using doubly deionized, Millipore filtered water. Semi-preparative and analytical HPLC (Vydac reversed-phase columns, TP201; column 1, 1 x 25 cm; column 2, 0.4 x 25 cm) were performed using a Hitachi L-7100 pump equipped with a gradient elution device and a Soma S-3702 variable wavelength UV detector which is connected to a PC computer installed with Hitachi HPLC analytical software. Mass spectra were determined with a Finnigan/Thermo

Quest MAT 95XL instrument operating in the electrospray ionization (ESI) mode in National Chung-Hsing University.

4.2 Chemical methods.

Synthesis of peptides and chlorambucil-peptide conjugates

Met-Hyp-Arg-Lys-(Py)₄-Lys-Arg-NH₂ (HyM-10)

This peptide was synthesized using solid phase methodology by manual operation of a Protein Technology PS3 peptide synthesizer. The first Fmoc-protected amino acid was coupled to the Nova Rink amide AM resin using PyBOP/NMM in DMF. All of the N_α-Fmoc-protected amino acids (in 4 equivalent ratio excess to the resin) were coupled in stepwise fashion using PyBOP/NMM in DMF after deprotection of the N-Fmoc group by piperidine. The side chains of Arg, Lys were protected by the Pmc and Boc groups, respectively. After coupling the last N-terminal Fmoc-amino acid residue, the resin was treated with the cleavage reagent (0.75 g phenol, 10 mL TFA, 0.5 mL thioanisole, 0.25 mL EDT) for 1.5 h, and then lyophilized. The resin was washed with dry ether (2 x 30 mL), filtered, and then washed with 5% acetic acid (200 mL). The combined filtrate was lyophilized and the product purified by semi-preparative reversed-phase HPLC (column 1) using gradient elution. Eluent A: 5% MeCN, 95% H₂O, 0.1% TFA; Eluent B, 95% MeCN, 5% H₂O, 0.1% TFA. A linear gradient was achieved by increasing the MeCN content from eluent A to eluent

B in 30 minutes. t_R (column 2), 15.09 min. m.p. 148-151°C, $[\alpha]_D^{27}$ -25.56 (c 0.30, MeOH/H₂O, 1:1); ESIMS requires: 1318.56, found: 1319.0.

CLB-Met-Hyp-Arg-Lys-(Py)₄-Lys-Arg-NH₂ (CLB-HyM-10)

The Fmoc group of Fmoc-Met-Hyp-Arg(Pmc)-Lys(Boc)-(Py)₄-Lys(Boc)-Arg(Pmc)-Resin was removed by 20% piperidine in DMF and chlorambucil and PyBOP/NMM (in 4 equivalent ratio excess to the resin) were added. The reaction was allowed to react for about 3 h, and the resin was treated with the cleavage reagent (0.75 g phenol, 10 mL TFA, 0.5 mL thioanisole, 0.25 mL EDT) for 1.5 h, and then lyophilized and purified as for peptide HyM-10. t_R (column 2), 18.91 min. m.p. 165-169°C, $[\alpha]_D^{24}$ -32.14 (c 0.9, H₂O); ESIMS calcd. 1604.75, found: 1605.0.

CLB-Gln-Hyp-Arg-Lys-(Py)₄-Lys-Arg-NH₂ (CLB-HyQ-10)

The Fmoc group of Fmoc-Gln-Hyp-Arg(Pmc)-Lys(Boc)-(Py)₄-Lys(Boc)-Arg(Pmc)-Resin was removed by 20% piperidine in DMF and chlorambucil and PyBOP/NMM (in 4 equivalent ratio excess to the resin) were added. The reaction was allowed to react for about 3 h, then worked up and purified as for CLB-HyM-10. t_R (column 2), 17.32 min, m.p. 163-166°C, $[\alpha]_D^{24}$ -23.08 (c 0.87, H₂O); ESIMS calcd. 1599.8, found: 1601.0.

4.3 DNase I footprinting

Full protocols for footprinting experiments have been published previously.^{11,14,15}

4.4 DNA cleavage induced by CLB-peptide conjugates

Radiolabeled pBR322 DNA fragments: 158-mer DNA duplex (upper strand 5'-³²P-labeled) and 135-mer DNA duplex (lower strand 5'-³²P-labeled) were prepared by PCR amplification in a thermal cycler (ABI model 9700) as previously described. The concentrations of DNA as determined by UV spectroscopy were around 10⁻⁷ M. Reactions were conducted in a total volume of 10 μL. Briefly, radiolabeled DNA (2 μL) was mixed with varying concentrations of 2 μL of CLB-HyM-10 or CLB-HyQ-10 dissolved in 5 mM sodium cacodylate buffer (pH 6.5) and the reaction allowed to proceed at 37°C for 30 min, cooled on ice, ethanol-precipitated, and lyophilized. Samples were heated at 90°C for 4 min prior to electrophoresis.

4.5 MALDI-TOF mass spectrometry

Measurements were performed with a Microflex MALDI mass spectrometer (Bruker Daltonik GmbH, Leipzig, Germany). 20 μL 40 μM U4A-L4T (duplex) in 5 mM sodium cacodylate buffer, pH 6.5 and 20 μL 4 μM CLB-peptide conjugate in the same buffer were mixed with a pipette and vortexed for 3 seconds, and centrifuged at 10,000 rpm for 10 seconds. The mixture was incubated at 37°C for 30 min. To this

was added 1 mL 99% alcohol and 5 μ L NaOAc (3M, pH 5.2), and the mixture was centrifuged at 10,000 rpm for 10 seconds. The product was stored at -20°C overnight, then centrifuged at 4°C at 14,000 rpm for 30 min. The ethanol was removed and 1 mL ethanol was again added and the mixture centrifuged at 4°C at 14,000 rpm for 10 min. This treatment was repeated twice and finally the ethanol was removed by a speedvac (800 rpm) at 25°C for 5 min. 1 mL 0.5 M trihydroxyacetophenone (THAP) in methanol was prepared. The matrix was prepared by adding 40 μ L 0.5 M diammonium hydrogen citrate (H_2O) to 100 μ L 0.5 M trihydroxyacetophenone (THAP) in methanol. 2.5 μ L of the matrix was introduced to the plate and allowed to dry for 3 min in air. To this matrix layer was added 1 μ L of a mixture of fresh matrix and reacted DNA sample (1:1). After 3 min the sample was subjected to MALDI-TOF analysis with 45% laser power, 400 ns delay time, 100 shots, using a linear and positive ion mode.

4.6 Circular dichroism (CD) studies

CD spectra were measured at 37°C with a Jasco J-815 instrument in the Institute of Chemistry, Academia Sinica. The duplex DNA was adjusted to 1.0 μM in 5 mM sodium cacodylate buffer (pH 6.5) and peptides, dissolved in the same buffer, were added to maintain final concentrations of 0.2, 1.0, 2.2, 2.4, 2.6, 2.8, 3.0, 3.2, 3.4, 4.0,

5.0 μM . Spectra were recorded after 60 min incubation at 37°C.

4.7 Isothermal titration calorimetry

ITC experiments were performed using a Microcal VP-ITC (MicroCal, Northampton, MA) with a reaction cell volume of 2 mL for oligonucleotide duplex (U4A-L4T) at 25°C or other temperatures as indicated in Table 3 and all samples were degassed under vacuum for 5 min. The DNA solutions at appropriate concentration in 5 mM sodium cacodylate, pH 6.5 (Table 3) were placed in the calorimeter cell and the peptide at appropriate concentration in 5 mM sodium cacodylate, pH 6.5 (273 μL) was placed in the titration syringe and injected in aliquots of 7 μL with 220 s intervals between the individual injections and stirring at 304 rpm, for a total of 39 injections. Data acquisition and analysis were performed using nonlinear least-squares fitting algorithm software (single site binding model, Microcal Origin 7.1 software). The K_a values were obtained from the ITC instrument by computer fit of the ITC isotherms and the corresponding ΔG values were calculated from the equation:

$$\Delta G = -RT \cdot \ln K_a$$

References

1. Sigman, D. S., Mazumder, A., Perrin, D.M. Chemical nuclease. *Chem. Rev.*, 1993, **93**, 2295-2316. Gallagher, J., Chen, C-H. B., Pan, C.Q., Perrin, D.M., Cho, Y.M., Sigman, D.S.; Optimizing the targeted chemical nuclease activity of 1,10-phenanthroline-copper by ligand modification. *Bioconjugate Chem.*, 1996, **7**, 413–420.
2. Dervan P.B. Design of sequence-specific DNA-binding molecule. *Science* 1986, **232**, 464–471; Schultz P.G., Dervan P.B. Distamycin and penta-N-methylpyrrololecarboxamide binding sites on native DNA. A comparison of methidiumpropyl-EDTA-Fe(II) footprinting and DNA affinity cleaving. *J Biomol Struct Dyn.* 1984, **1**, 1133–1147.
3. Routier, S., Vezin, H., Lamour, E., Bernier, J.L., Catteau, J.P., Bailly, C. DNA cleavage by hydroxylsalicylidene-ethylenediamine-iron complex. *Nucleic Acids. Res.*, 1999, **27**, 4160-4166.
4. Cheng. C.C., Huang-Fu, W.C., Hung, K.C. Chen, P.J., Wang, W.J., Chen, Y.J. Mechanistic aspects of $\text{Co}^{\text{II}}(\text{HAPP})(\text{TFA})_2$ in DNA bulge-specific recognition. *Nucleic Acids. Res.*, 2003, **31**, 2227-2233.
5. Qian Li, Q., Browne, W.R., and Roelfes, G. (2011) DNA cleavage activity of $\text{Fe}(\text{II})\text{N}_4\text{Py}$ under photo irradiation in the presence of 1,8-Naphthalimide and 9-Aminoacridine: Unexpected effects of reactive oxygen species scavengers *Inorg. Chem.* **50**, 8318–8325.
6. Takimoto, C.H., Calvo, E. in Principles of oncologic pharmacotherapy in cancer management: a multidisciplinary approach. Pazdur, R., Wagman, L.D., Camphausen, K.A., Hoskins, W.J. Eds., 2008, 11th edition.
7. Rai, K.R., Peterson, B.L., Appelbaum, F.R., Kolitz, J., Elias, L., Shepherd, .L,

Hines, J., Threatte, G.A., Larson, R.A., Cheson, B.D., Schiffer, C.A. Fludarabine compared with chlorambucil as primary therapy for chronic lymphocytic leukemia. *N. Engl. J. Med.*, 2000, **343**, 1750-1757.

8. Sheh, L., Chang, H.W. Ong, C.W., Chen, S.L., Bailly, C., Linssen, Waring, M.J. Synthesis, DNA binding, and sequence specificity of DNA alkylation by some novel cyclic peptide-chlorambucil conjugates. *Anti-Cancer Drug Des.*, 1995, **10**, 373-388.

9. Minnock, A., Lin, L.S., Morgan, J., Crow, S.D.G., Waring, M.J., Sheh, L. Sequence-specific DNA cleavage by dipeptides disubstituted with chlorambucil and 2,6-dimethoxyhydroquinone-3-mercaptoacetic acid. *Bioconjugate Chem.*, 2001, **12**, 870-882.

10. Bailly, C. Personal communications.

11. Chang, J.C., Yang, C.H., Chou, P.J., Yang, W.H., Chou, I.C., Lu, C.T., Lin, P.H., Hou, R.C.W., Jeng, K.C.G., Cheng, C.C., and Sheh, L. DNA sequence-specific recognition of peptides incorporating the HPRK and polyamide motifs. *Bioorg. Med. Chem.*, 2004, **12**, 53-61.

12. Yang, C.H., Chen, W.F., Jong, M.C., Jong, B.J., Chang, J.C., Waring, M.J., Ma, L., Sheh, L. Semiquinone footprinting. *J. Am. Chem. Soc.*, 2004, **126**, 8104-8105.

13. Yang, C.H., Jeng, K.C.G., Yang, W.H., Chen, Y.L., Hung, C.C., Lin, J.W., Chen, S.T., Richardson, S., Martin, C.R.H., Waring, M.J., Sheh, L. Unusually strong positive cooperativity in binding of peptides to latent membrane protein-1 DNA fragments of the Epstein-Barr viral gene. *ChemBioChem*, 2006, **7**, 1187-1196.

14. Kao, K.L., Huang, J.C.T., Yang, C.K., Jeng, K.C.G., Chang, J.C., Yao, W.C.,

Hsien, S.C., Waring, M.J., Chen, M.H., Ma, L., Sheh, L. Detection of multiple network-based allosteric interactions between peptides and arrays of DNA binding sites. *Bioorg. Med. Chem.*, 2010, **18**, 366-376; Huang, J.T.B., Yang, R.C.K., Hung, W.K., Waring, M.J., Sheh, L. in *Molecular Recognition*, J.A. McEvoy ed., 2011 Nova Science Publishers Inc., New York, ISBN 978-1-61122-734-5, open access available.

15. Huang, J.T.B., Chen, Y.C., Chang, J.C., Jeng, K.C.G., Kao, K.L., Yang, C.K., Kan, L.S., Wey, M.T., Waring, M.J., Chen, C.S., Chien, W.J., Sheh, L. Novel DNA-peptide interaction network. *Bioorg. Med. Chem.*, 2010, **18**, 2575-2585.

16. Yang, R.C.K., Huang, J.T.B., Chien, S.C., Huang, R., Jeng, K.C.G., Chen, Y.C., Liao, M., Wu, J.R., Hung, W.K., Hung, C.C., Chen, Y.L., Waring, M.J., Sheh, L. Energetic Studies on DNA-peptide interaction in relation to the enthalpy-entropy compensation paradox. *Org. Biomol. Chem.*, 2013, **11**, 48-61.

17. Eck, M.J., Sprang, S. The structure of tumor necrosis factor- α at 2.6 angstrom resolution. *J. Biol. Chem.* 1989, **264**, 17595-17605 and reference quoted therein.

18. N.M. Luscombe, N.M., Laskowski, R.A., Thornton, J.M. Amino acid-base interactions: a three dimensional analysis of protein-DNA interactions at an atomic level. *Nucleic Acids Res.*, 2001, **29**, 2860-2874.

19. Buchmueller, K.L., Staples, A.M., Howard, C.M., Horick, S.M., Uthe, P.B., Le Minh, N., Cox, K.K., Nguyen, B., Pacheco, K.A.O., Wilson, W.D., Lee, M. Extending the language of DNA molecular recognition by polyamides: unexpected influence of imidazole and pyrrole arrangement on binding affinity and specificity. *J. Am. Chem. Soc.* 2005, **127**, 742-750.

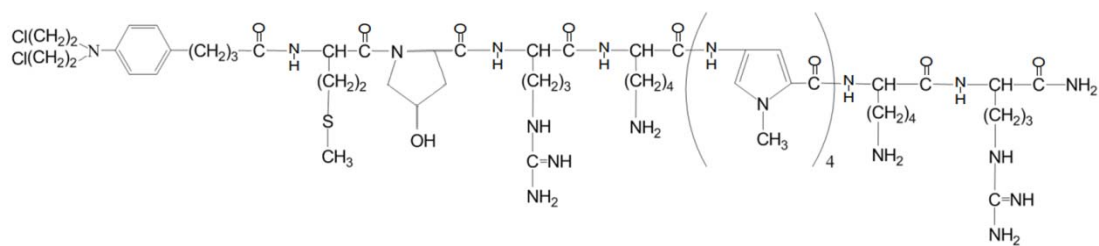
20. Brown, T., Mackay, H., Turlinton, M., Sutterfield, A., Smith, T., Sielaff, A., Westrate, L., Bruce, C., Kluza, J., O'Hare, C., Nguyen, B., Wilson, W.D., Hartley, J.A., Lee, M. Modifying the N-terminus of polyamides: PyImPyIm has improved

- sequence specificity over f-ImPyIm. *Bioorg. Med. Chem.*, 2008, **16**, 5266-5276.
21. Sheppard, T.L., Ordoukhanian, P., Joyce, G.F. A DNA enzyme with N-glycosylase activity. *Proc. Natl. Acad. Sci. U.S.A.*, 2000, **97**, 7802-7807.
22. Schwartz, P.A., Verticatt, M.J., Schramm, V.L. Transition state analysis of the arsenolytic depyrimidination of thymidine by human thymidine phosphorylase. *Biochemistry*, 2011, **50**, 1412-1420.
23. Breslauer, K.J., Rometa, D.P., Chou, W.Y., Ferrante, R., Curry, J., Zaunczkowski, D., Snyder, J.G., Marky, L.A. Enthalpy-entropy compensations in drug-DNA binding studies. *Proc. Natl. Acad. Sci. U.S.A.*, 1987, **84**, 8922-8926.
24. Dixit, S.B.; Andrews, D.Q.; Beveridge, D.L.; Induced fit and the entropy of structural adaptation in the complexation of CAP and λ -repressor with cognate DNA sequence. *Biophys. J.* **2005**, *88*, 3147-3157.
25. Williams, D.H., E. Stephens, O'Brien, D.P., Zhou, M. Understanding noncovalent interactions: ligand binding energy and catalytic efficiency from ligand-induced reductions in motions within receptors and enzymes. *Angew. Chemie. Int. Ed.*, 2004, **43**, 6596-6616, and references cited therein.

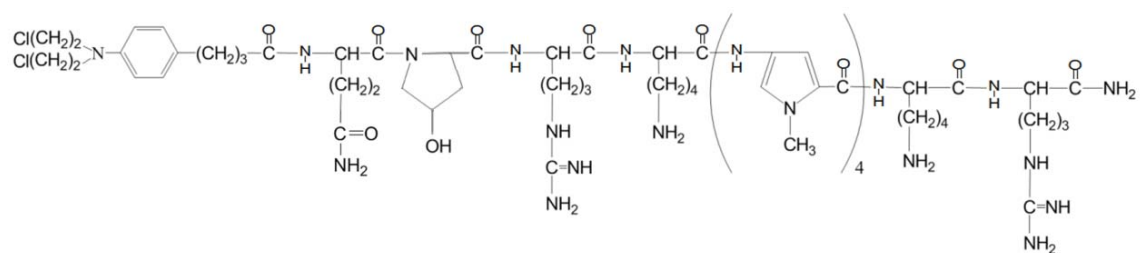
Table 1. Sequence-selective binding and cleavage by peptides and CLB-peptide conjugates on complementary 5'-³²P-labeled upper (158-mer) and 5'-³²P-labeled lower (135-mer) DNA strands.

Sequence-selective binding of peptides	K_a	n_H	Position of Interstrand bidentate interactions	Sequence-selective Cleaved fragments of CLB-peptide conjugates
HyM-10 5'-AAATACCG-3' (U84-90)	3.5×10^6	1.1	84-85	CLB-HyM-10 5'-CGGTGTGAAA-3' (U76-85)
5'-GGAGAAAATACCG-3' (U104-115)	3.4×10^6	2.4	105-111	5'-GTAAGGAGAAAA-3' (U100-111)
5'-TTTCACAC-3' (L85-78)	5.0×10^7	1.9		5'-TATG-3' (L73-70)
5'-TTTTCTCCTTA-3' (L111-101)	1.0×10^7	2.1		5'-CACCG-3' (L80-77)
				5'-GTGCGGTA-3' (L93-86)
				5'-GGTA-3' (L115-112)
HyQ-10 5'-AAATACCG-3' (U83-90)	3.8×10^6	2.7	83-86	CLB-HyQ-10 5'-GGTGTGAA-3' (U77-85)
5'-GAAAATACCG-3' (U107-116)	5.6×10^6	3.6	107-112	5'-TAAGGAGAAAA (U101-111)
5'-ATTTACAC-3' (L86-80)	2.9×10^6	3.7		5'-GGCGCT-3'(U121-127)
5'-ATTTTCTCCTT-3' (L112-102)	5.7×10^6	1.8		5'-GTGCGGTA-3' (L93-86)

K_a and n_H are the apparent association constant and Hill coefficient determined from concentration-dependent DNase I footprinting studies, respectively. The binding site positions on the upper and lower strands are abbreviated as U and L, respectively.



CLB-HyM-10



CLB-HyQ-10

Table 2. Cleavage fragments most frequently detected in MALDI-TOF experiments with DNA duplexes and bound CLB-peptide conjugate.

Mass	Cleavage fragments	Proposed cleavage mechanism
998		Depyrimidination of T ₁₇
1442		Depurination of A ₅
1598		Depurination of A ₁₆ and depyrimidination of T ₂₂
1732		Depurination of G ₆
1948		Depyrimidination of C ₂₁ and depurination of G ₁₄
2033		Depyrimidination of T ₁₈ and T ₂₅
2337		Depurination of G ₃ and depyrimidination of T ₁₁
2643		Depyrimidination of T ₁ and depurination of A ₁₀
2944		Depurination of G ₁₄ and depyrimidination of C ₂₄

5'-T₁-A₂-G₃-G₄-A₅-G₆-A₇-A₈-A₉-A₁₀-T₁₁-A₁₂-C₁₃-3'

5'-A₁-A₂-G₃-G₄-A₅-G₆-A₇-A₈-A₉-A₁₀-T₁₁-A₁₂-C₁₃-3

3'-A₂₆-T₂₅-C₂₄-C₂₃-T₂₂-C₂₁-T₂₀-T₁₉-T₁₈-T₁₇-A₁₆-T₁₅-G₁₄-5'

3'-T₂₆-T₂₅-C₂₄-C₂₃-T₂₂-C₂₁-T₂₀-T₁₉-T₁₈-T₁₇-A₁₆-T₁₅-G₁₄-5'

Duplex U4A-L4T

Duplex XU4A-XL4T

For details of MALDI-TOF mass fragments, see Figures 4, panels A-H and Supporting Information, Tables [Ia]-[Id].

Table 3. Comparison of thermodynamic parameters from titration of peptides, chlorambucil-peptide conjugates, and drugs versus DNA duplexes.

Entry	Peptide/conjugate (mM)	[DNA] (mM)	ΔH (kcal/mol)	ΔS (cal/mol)	ΔG (kcal/mol)	$T\Delta S$ (kcal/mol)	K_a (M^{-1})
1	HyM-10(0.15)	0.0033	-50.5	-140	-8.8	-41.7	2.9×10^6
2	HyQ-10(0.15)	0.01	-74.4	-221	-8.6	-65.9	1.9×10^6
3	HyH-10 (0.05)	0.0033	-51.2	-142	-8.8	-42.3	2.9×10^6
4	HyS-10 (0.15)	0.006	-31.2	-74.5	-9.0	-22.2	4.2×10^6
1a	CLB-HyM-10(0.15)	0.005	-25.4	-56.3	-8.6	-17.8	2×10^6
2a	CLB-HyQ-10(0.15)	0.007	-46.0	-126	-8.3	-37.5	1.2×10^6
3a	CLB-HyH-10(0.15)	0.005	-30.4	-75	-8.0	-22.4	7.7×10^5
4a	CLB-HyS-10(0.15)	0.005	-26.6	-63.1	-7.8	-18.8	5.3×10^5
	Netropsin	-	-11.2	+5	-12.7	-	-
	Distamycin A	-	-18.5	-20	-12.6	-	-

Peptides HyM-10, HyQ-10, HyH-10, HyS-10 and corresponding CLB-peptide conjugates were titrated against oligonucleotide duplex (U4A-L4T) employing isothermal titration calorimetry. Netropsin and distamycin A were titrated versus copolymer duplex poly[d(A-T)]•poly[d(A-T)] using batch calorimetry.²²

The amino acid sequence of the peptides are:

Met-Hyp-Arg-Lys-(Py)₄-Lys-Arg-NH₂ (HyM-10)

Gln-Hyp-Arg-Lys-(Py)₄-Lys-Arg-NH₂ (HyQ-10)

His-Hyp-Arg-Lys-(Py)₄-Lys-Arg-NH₂ (HyH-10)

Ser-Hyp-Arg-Lys-(Py)₄-Lys-Arg-NH₂ (HyS-10)

Conjugation of chlorambucil to the *N*-terminal of these peptides afforded corresponding CLB-peptide conjugates.

Legends

Figure 1. Plots comparing the susceptibility of 158-mer (upper strand) and 135-mer (lower strand) of pBR322 DNA fragment to cleavage induced by CLB-peptide conjugates, or by DNase I (footprinting) in the presence of peptides: A, CLB-NR6; B, CLB-HyM-10; C, peptide HyM-10; D, CLB-HyQ-10; E, peptide HyQ-10. The vertical dotted lines in Figure 1 C and Figure 1E denote the positions of interstrand bidentate interactions between peptide moieties and bases of DNA. F, G: Representative cleavage of the pBR322 DNA fragment induced by CLB-HyM-10 and CLB-HyQ-10 at 900 nM and 1800 nM, respectively.

Figure 2. Autoradiographs showing cleavage of 158-mer (left panels) and 135-mer (right panels) of pBR322 DNA fragment induced by DNase I (footprinting) in the presence of peptide HyM-10 (upper panels), or induced by incubating with conjugate CLB-HyM-10 in 5 mM sodium cacodylate buffer (pH 6.5) at 37°C for 30 min (lower panels).

Figure 3. Panel A: CD spectrum for the titration of duplex U4A-L4T versus peptide HyM-10 at peptide concentrations of 0.5, 1.0, 2.2, 2.4, 2.6, 2.8, 3.0, 3.2, 3.4, 4.0, 5.0, 7.0 μM at 37°C. Panel B: Corresponding CD difference spectra with the contribution of free duplex and peptide HyM-10 subtracted. Panel C: Titration of U4A-L4T versus conjugate CLB-HyM-10 at conjugate concentrations of 0.5, 1.0, 1.5, 1.8, 2.1, 2.2, 2.3, 2.4, 2.5, 2.6, 2.7, 2.8, 3.0, 3.5, 4.0, 5.0 μM at 37°C. Panel D: Corresponding difference spectra with the contribution of free duplex and conjugate CLB-HyM-10 subtracted. Panel E: Job's plots of $\Delta\theta \cdot X$ versus mole fraction ligand at 322 nm (X = mole fraction ligand) for the titration of duplex U4A-L4T versus different ligands. The stoichiometry of ligands HyM-10, HyQ-10, CLB-HyM-10, and CLB-HyQ-10 binding to duplex U4A-L4T is determined to be 3:1, 3:1, 2:1, 2:1, respectively.

Figure 4. Major cleavage fragments induced by conjugates CLB-HyM-10, (panel A) and CLB-HyQ-10 (panel B) on the oligonucleotide duplex U4A-L4T; major cleavage fragments induced by conjugates CLB-HyM-10, (panel C) and by CLB-HyQ-10 (panel D) on the oligonucleotide duplex XU4A-XL4T as detected by MALDI-TOF mass spectroscopy; representative MALDI-TOF mass peaks of major cleavage fragments induced by conjugates CLB-HyM-10, (panel E) and CLB-HyQ-10 (panel F) on the oligonucleotide duplex U4A-L4T. The sequences of the upper and lower strands of duplexes U4A-L4T and XU4A-XL4T are shown in Table 2.

Figure 5A. Proposed stepwise cleavage of duplex U4A-L4T induced by chlorambucil-peptide conjugate CLB-HyM-10 via an initial monomeric binding, followed by a dimeric binding mode, resulting in the generation of fragmental strands from opposite strands. Figure 5B, Proposed stepwise cleavage of duplex U4A-L4T induced by conjugate CLB-HyQ-10 via a similar dimeric binding mode. Before DNA cleavage, the peptide moieties of the conjugate first interact with the DNA minor groove via monodentate, interstrand bidentate, ionic and hydrophobic interactions (non-covalent interactions not shown). Figure 5C. Proposed stepwise cleavage mechanism of duplex XU4A-XL4T induced by chlorambucil-peptide conjugate CLB-HyM-10. Figure 5D. Proposed stepwise cleavage mechanism of duplex XU4A-XL4T induced by conjugate CLB-HyQ-10. X, M, Q, Ph, Py and dr represent residues of chlorambucil, methionine, glutamine, hydroxyproline, 4-amino-1-methylpyrrole-2-carboxylic acid, and deoxyribose, respectively. Position of DNA cleavage is proposed to locate near the CLB moiety and is denoted by the red arrow sign ↓. The underlined base indicates where depurination or depyrimidination has occurred. The found mass of the cleaved fragments from MALDI-TOF experiments are as shown in brackets.

Figure 6A. ITC curves for titration of decapeptides HyM-10, HyQ-10, CLB-HyM-10

and CLB-HyQ-10 into the U4A-L4T duplex at 25°C. For each experiment the top panel represents the raw heat of binding generated with successive additions of peptide, and in the bottom panel the integrated heat is plotted versus peptide/DNA molar ratio. Data acquisition and analysis were performed using nonlinear least-squares fitting algorithm software (Microcal Origin 7.1).

Figure 6B. Plot of enthalpy (ΔH) versus entropy ($T\Delta S$) from ITC of HyM-10, HyQ-10, CLB-HyM-10 and CLB-HyQ-10 added to the U4A-L4T duplex at 25°C (298 K).

Figure 6C. Plot of enthalpy (ΔH) versus entropy ($T\Delta S$) from ITC of HyM-10 [1], HyQ-10 [2], HyH-10 [3], HyS-10 [4], CLB-HyM-10 [1a], CLB-HyQ-10 [2a], CLB-HyH-10 [3a], CLB-HyS-10 [4a] added to the U4A-L4T duplex at 25°C (298 K).

Figure 6D. Three-dimensional plot of ΔH , $T\Delta S$, ΔG from titration of peptides and CLB-peptide conjugates into the U4A-L4T duplex. The short vertical projection plane (in green) corresponds to ΔG magnitudes preserved around -7.9 kcal/mol. The figure represents a view of the 'cube' from below.